Density-functional calculations of the structural properties of tin under pressure

N. E. Christensen*
Institute of Physics and Astronomy, Aarhus University, DK-8000 Aarhus C, Denmark

M. Methfessel
Institut für Halbleiterphysik, Walter-Korsingstrasse 2, OD-1200 Frankfurt/Oder, Germany
(Received 7 October 1992; revised manuscript received 22 March 1993)

Total-energy calculations within the local-density approximation (LDA) to the density-functional theory are used to study the properties of tin under pressure. It is known experimentally that the cubic diamond structure (α) is stable at zero pressure and low temperature, but the application of a very small pressure, a few kbar, drives Sn into the β-Sn structure. The transition is accompanied by a large volume reduction, $\approx 20\%$. This is also found in the present calculations, and they further suggest that the β structure is stable for pressures up to ≈ 100 kbar, above which Sn transforms into a body-centered-tetragonal phase. Experiments carried out at room temperature yield a transition pressure of 95 kbar, and extrapolating the phase diagram from 0 °C to $T=0$ K the experimental zero-temperature value is estimated to be 120–130 kbar. At $T=0$ and $P\approx 105$ kbar the calculation predicts the structure to be bct with $c/a=0.91$. At finite temperatures the c/a ratio in this phase is expected to range from 0.85 to 1.06, but with increasing pressure a predominance of structures with $c/a=1.00$ is predicted. Above 300–400 kbar the structure may be characterized as bcc (i.e., $c/a=1.00$ is clearly dominating), and for pressures up to at least 2 Mbar the bcc phase remains the phase with the lowest enthalpy when compared with α, β, bct, fcc, sc, hcp, dhcp, and primitive hexagonal structures. The bct$\rightarrow$bcc transition is of first order at $T=0$. The pressure dependence of the Γ_5 and Γ_3 phonons in β-Sn is calculated, and agreement with recent Raman measurements is obtained.

I. INTRODUCTION

The electronic and structural properties of tin have been of considerable interest to experimental[1–8] as well as theoretical[9–15] solid-state physics over several decades. The reason is that its properties depend sensitively on external parameters like temperature (T) and pressure (P), and this is rather unusual for an elemental solid. Tin belongs to group IV of the periodic table and has as such, like its partners C, Si, Ge, and Pb, a tendency to form sp^3 bonds. But, going down rowwise, one finds that the sp^3 bond order decreases[16] and that the $s\rightarrow p$ promotion energy simultaneously increases. It so happens that Sn is at the borderline where the gain in energy obtained by forming sp^3 bonds hardly exceeds the energy cost associated with the transfer of an electron from an s state to a p state. Thus, above Sn, the group-IV elements (Ge, Si, and C) tend to form strongly tetrahedrally bonded crystals, whereas this is not the case below (Pb, which prefers the fcc structure). Relativistic dehybridization[16,17] plays an important role in this connection, as also follows from Fig. 1.

Tin does assume the diamond structure, but only at low pressures and low temperatures. At atmospheric pressure this α form is stable below 13 °C (grey tin), whereas the usual metallic "white tin" is the modification observed at higher temperatures and pressures. Its crystal structure is named after this tin phase, β-Sn, which is derived from a body-centered tetragonal Bravais lattice and has two atoms in the basis, (0,0,0) and $(a/2,0,c/4)$. The atomic volume of β-Sn is only 80% of that of α-Sn. Experiments[6] show that the β structure is stable for pressures up to 95 kbar. Above this Sn tends to form the body-centered cubic (bcc) structure. This, however, is only achieved at very high pressures, above 400–500 kbar. In the pressure range between 95 and 400 kbar the structure has been described as body-centered tetragonal

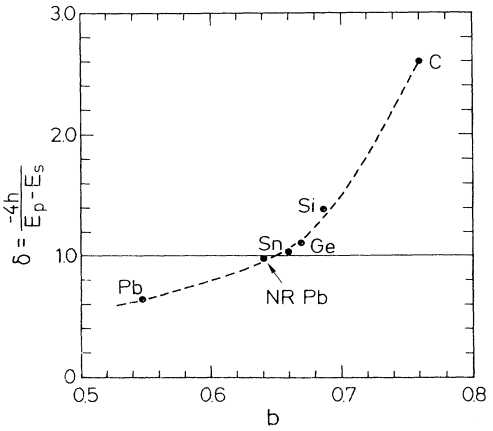

FIG. 1. Group-IV elements: Calculated ratio δ, between the sp^3 bond formation energy and the $s\rightarrow p$ promotion energy cost as a function of bond order, b (see Refs. 16 and 24). The calculations are relativistic, except the one labeled "NR Pb" which is a fully nonrelativistic calculation for lead (further discussion in Ref. 16).

(bct). The bct structure has a large c/a ratio, ≈ 0.90. This peculiarity, i.e., that Sn does not go directly to the highly coordinated bcc structure, but assumes a bct structure with large c/a ratio, was explained[18] as a consequence of the splitting of the bcc H_{15}-level (just below the Fermi level) under tetragonal strain. Olijnyk and Holzapfel[6] observed, in a certain pressure range, the coexistence of bct and bcc structures, and only above 500 kbar did they characterize the samples as purely bcc. This is in agreement with the present calculations, which, however, predict that a range of c/a ratios should be observed (at room temperature) also at lower pressures. The simultaneous occurrence of bct and bcc structures is a consequence of an extremely low barrier in total energy between them, a barrier that is much smaller than the thermal energy $k_B T$ at the temperature at which the experiments were performed. The bcc structure appears to be stable up to very high pressures, 1.2 Mbar at least, according to the experiments by Desgreniers, Vohra, and Ruoff.[19] It has been suggested that a bcc→hcp transition might occur in Sn at very high pressures. The experiments of Ref. 6 did not confirm this, but as pointed out there,[6] the experiments carried out at room temperature could not exclude that such a transition could take place at low temperatures. Our calculations suggest that the bcc→hcp transition indeed cannot occur. Neither is a transition to the fcc structure possible. We also include the primitive cubic (sc) and hexagonal (phex) structures as well as the double-hexagonal close packed (dhcp) structure in the present study. Also these have higher enthalpy than bcc-Sn at all positive pressures, at least up to 2 Mbar, the upper pressure limit in our calculations.

The most detailed theoretical study of the structural properties of Sn under pressure was published very recently by Cheong and Chang.[14] They performed calculations within the local-density approximation (LDA) to the density functional theory (as we do also). They found the transition sequence β-Sn→bct→bcc consistent with experiment. The transition pressures, though, differ somewhat from experimental values. This is not surprising in view of the very small values of the total-energy differences involved. For such a sensitive system it is especially important to perform calculations by means of different methods. Our results are in many respects similar to those of Ref. 14, but differences exist in numerical detail. The calculations of Ref. 14 indicate that the bcc→hcp transition *does* occur, but the energy differences involved are so small that numerical errors may affect the conclusion. Cheong and Chang used the norm-conserving *ab initio* pseudopotential method, and it is possible that this becomes less accurate at strongly reduced volumes due to core overlap.

We apply the full-potential linear muffin-tin-orbital (LMTO) method.[20–22] This has the advantage that a very small basis set is needed, and its application is not limited to cases without d and f states in the band structure. The LMTO basis set can be chosen such that the accuracy where it can be tested (sp materials) is at least as good as the *ab initio* pseudopotential calculations.

Some details of the calculation method are given in Sec. II, and we discuss in particular the importance of treating the corelike Sn-4d states as valence-band states. It is shown here that the energy of these states relative to the other valence band is a critical parameter in determining delicate structural energy differences. Also, we examine the effects of including the spin-orbit coupling and, of particular interest to the applications of the LMTO method, we examine the accuracy of the atomic-sphere approximation[20] (ASA). The transition pressures as well as characteristic parameters, such as lattice constants, bulk moduli, c/a ratios are given in Sec. III. The calculated Γ_3 and Γ_5 phonon frequencies and mode Grüneisen parameters are discussed in Sec. IV, whereas Sec. V gives a short summary.

II. CALCULATIONAL METHOD

Some of the structural energy differences that we need to calculate are very small, ≈ 1 mRy or less. This is, in particular, the case for the "frozen-phonon" calculations in Sec. V. This means that the calculational scheme must be numerically very accurate. The pseudopotential method as used in Ref. 14 is well suited for the LDA calculations for Sn (and semiconductors). The plane-wave basis set can be kept relatively small for these materials, and the nonspherical charge distribution is accurately described. We wish to use the linear muffin-tin-orbital (LMTO) method[20] because it uses a small basis set. This implies that the matrix dimensions are considerably smaller than in the case of the pseudopotential scheme, and we can therefore sample within reasonable computing times large numbers of points in k space. This reduces Brillouin zone integration errors. A density of k points corresponding to more than 500 points in the irreducible bcc wedge is needed. The bcc and bct structures are calculated with the same (bct) zone in order to obtain cancellation of numerical errors. The number of k points was in all cases increased until the energy differences could be considered sufficiently free of integration errors, less than 10 μRy. The exchange-correlation terms are calculated in the LDA using the parametrization by von Barth and Hedin.[23]

The version of the LMTO method most frequently used employs the atomic-sphere approximation (ASA). Within the ASA, total energies are obtained from a functional with potentials and charge densities that are made spherically symmetric inside space-filling atomic spheres. The ASA has been surprisingly successful for many applications, sometimes with inclusion of "combined correction" terms,[20] and, for open structures, with introduction of "empty spheres."[24–26] According to experience we expect that bct-bcc structural energy differences, elastic constants and phonon frequencies cannot be calculated within the ASA, but require application of a method that retains the nonspherical shape of the charge distribution.[27,28] The results presented in the subsection below confirm this. We therefore use the full-potential LMTO method as implemented by Methfessel and coworkers.[21,29] This still contains "spheres," but now only to define the basis set, the region in which the envelope functions are augmented. The spheres are also used as fix surfaces in the interpolation[21] of the nonspherical charge

densities. But, apart from these applications of "spheres" (which do not overlap), there are no shape approximations. In order to obtain sufficient accuracy the basis set is expanded in comparison with usual LMTO-ASA calculations. The latter usually employs (for semiconductors) s, p, and d states on real-atom sites as well as interstitial positions.[25,24] But only one type of envelope function[20] is used. This is for convenience taken to be the one corresponding to the interstitial kinetic energy κ^2 equal to zero. The FP-LMTO basis set that we use here employs up to three κ values. On each Sn site we place s-, p-, and d-basis functions corresponding to three, three, and two κ values, respectively. In cases (like α-Sn) where empty spheres are used, no orbitals are, nevertheless, needed on these sites. Consequently, the basis has 22 functions per Sn atom, and empty spheres are only used to obtain sufficient accuracy in the density fit between the "atoms." Basis-set convergence was checked by increasing their size, and by varying the muffin-tin-radii. The result of these convergence tests is that the basis set described gives the accuracy needed for comparison of the various high-pressure phases of Sn, and this agrees with the conclusion of a similar study of the structural and dynamical properties of Si.[22]

The relativistic shifts are included, but spin-orbit (SO) coupling is omitted, i.e., the calculations are scalar relativistic. Spin-orbit coupling does not shift the bands, to first order, it merely introduces level splittings. Thus, it is usually assumed that it does not affect total energy calculations noticeably. In some solids with heavy elements, like Pb, there may be an effect.[16] A preliminary investigation[30] indicated that the spin-orbit coupling does not affect the structural energy differences at $P=0$, but in view of the smallness of the energy differences we find it necessary to calculate the effects over a wide pressure range. This is done by performing fully Dirac-[31] and scalar-relativistic ASA calculations for α- and β-, as well as bct-Sn.

A. ASA calculations, spin-orbit coupling

The structural differences in free energy versus pressure are obtained by calculating the total energy E as a function of volume for each of the structures considered, derive the pressure P, and then the enthalpy,

$$H(P)=E+PV\ .$$

The minimum in the total-energy function, $E(V)$, has to be lowest for the α phase, but, in order to be consistent with observations, only slightly lower than that of β-Sn. The scalar-relativistic results illustrated in Fig. 2 obtained within the ASA already violates this requirement. This is mainly due to a difference in accuracy between the α calculations and the others in the ASA because the diamond structure includes "empty spheres." But it is seen that the β minimum is slightly below that of the bcc structure, and a $\beta\rightarrow$bct transition is predicted. Figure 3 shows the enthalpy variation with pressure, and it follows that the ASA scalar-relativistic calculation predicts the transition to occur around 500 kbar, but the transition is to bcc, i.e., $c/a=1.00$, which is in contrast to observations, and also in disagreement with the model calculation[32] in Ref. 18. Considering the magnitude of the total energy differences this error may at first not seem to be serious, but it does in fact reflect a fundamental difficulty in straight ASA calculations when applied to calculate small energy changes associated with symmetry-breaking distortions.[27] For Sn this is illustrated in Fig. 4, where the enthalpy, calculated within the ASA at the fixed pressure $P=200$ kbar for the bct structure is plotted as a function of c/a. A minimum close to $c/a=0.90$ is indeed found, but the enthalpy curve does not exhibit the proper symmetry around $c/a=1.00$ (bcc). The total energy should predict the bcc to be locally stable, i.e., an extremum should appear at $c/a=1.00$. This ASA error is observed at all pressures, and the ASA thus fails to predict correctly the bct$\rightarrow$bcc transition, and pure ASA cannot yield proper elastic shear constants for bcc-Sn.[27]

The entire calculation for α-, β-, and bct-Sn was re-

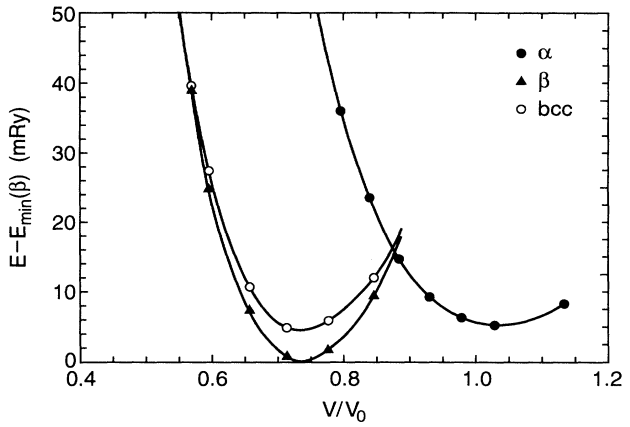

FIG. 2. Total energies of α-, β-, and bcc-Sn as functions of volume as calculated by means of the scalar-relativistic LMTO-ASA method. Two energy panels are used here; the Sn-4d states are included in a separate lower-energy panel.

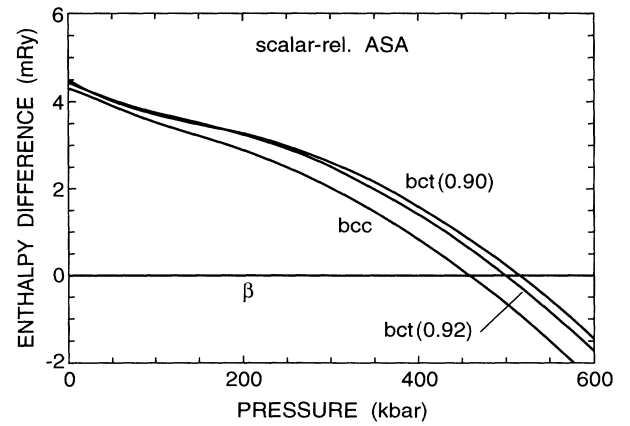

FIG. 3. Free energy of some bct phases of Sn, relative to β-Sn, as calculated by means of the scalar-relativistic LMTO-ASA method.

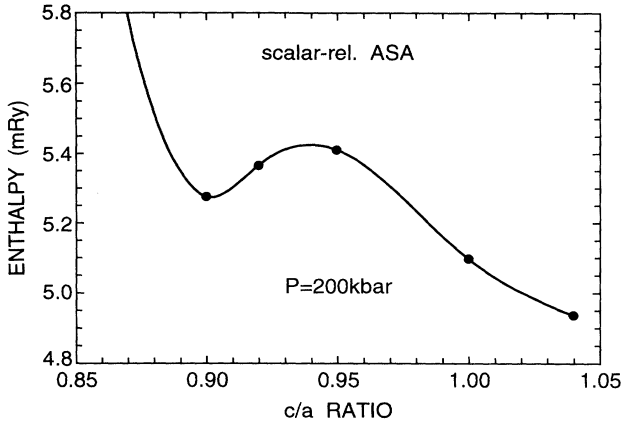

FIG. 4. LMTO-ASA calculation of the free energy (at $T=0$) of bct-Sn as a function of the axial c/a ratio. The pressure is fixed at $P=200$ kbar. Note that the curve does not exhibit a local extremum at $c/a=1$.

peated, still within the ASA, but using the Dirac-relativistic LMTO. This means that spin-orbit (SO) coupling is now also included, and not just as a perturbation. Figure 5 shows that Sn-α still is above the β phase [Fig. 5(b)]. The $\beta\rightarrow$bct transition occurs at a slightly higher pressure than in the scalar-relativistic case. But the SO correction to the transition pressure is marginal. Still,

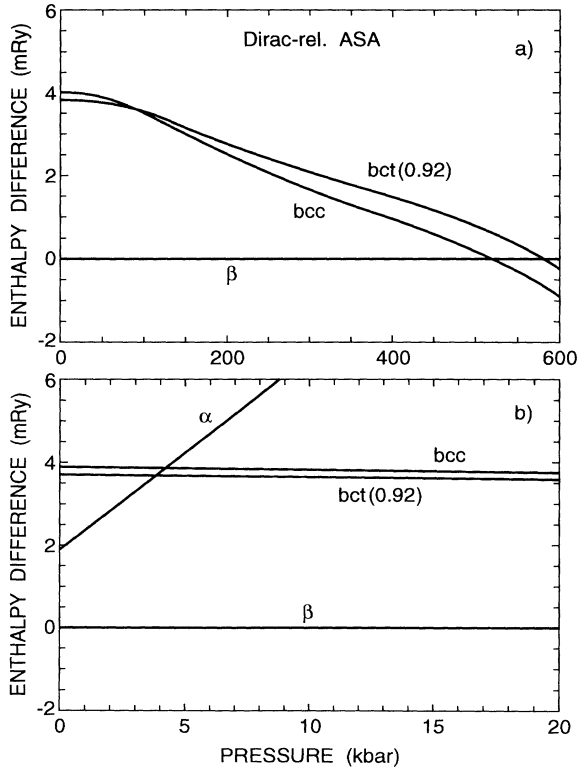

FIG. 5. Similar to Fig. 3 (i.e., still ASA), but using the Dirac-relativistic LMTO method. The low-pressure regime is shown in Fig. 3(b), which also includes the results for α-Sn.

the ASA error is present that predicts a $\beta\rightarrow$bcc transition rather than a transition to a tetragonal structure with c/a smaller than 1.

The calculations here show that for the purpose of calculating the delicate total-energy differences associated with the structural transformations in Sn we cannot rely on the accuracy of the ASA. The comparison between scalar- and Dirac-relativistic LMTO-ASA calculations suggest that the effects of the spin-orbit coupling on the predicted pressure-induced transitions are negligible.

The calculations of the structural properties of Sn under pressure are therefore calculated by means of the full-potential–linear-muffin-tin-orbital (FP-LMTO) method, and spin-orbit coupling is omitted, i.e., the calculations are scalar relativistic.

B. The Sn-4*d* states

The semicore like 4*d*-states lie low in energy, but reach so far into the outer part of the atom that they should be treated as "band states" on the same footing as the other valence states (compare also to the Ga-3*d* states[25] in GaAs). It is not sufficient to treat them as relaxed core states. The contribution to the cohesion from the 4*d* states becomes increasingly important as pressure is applied. Due to the finite range over which the linearization is accurate, this problem is usually treated in the LMTO by introducing several "energy panels" (see Fig. 6 of Ref. 25). We therefore first used two panels [the ASA calculations in subsection *A*, as well as the FP-LMTO calculation in Fig. 6(a)]. In a lower panel the linearization energies [$E_\nu(l)$] are in the Sn-4*d* band center, whereas $E_\nu(d)$ in the upper energy panel is located in the neighborhood of the bottom of the (unoccupied) 5*d* band [$E_\nu(d)$ cannot be allowed to adjust freely to the center-of-gravity of the occupied part of the upper valence bands due to occurrence of nonphysical bands at certain volumes]. Figure 6(a) shows this type of LMTO calculation yields very good relative positions of the energy-volume curves for the β- and α-Sn phases, but the total energies for the bct and bcc [only bcc is shown in Fig. 6(a)] lie too low, their minima being between those of α- and β-Sn. Consequently, the energy of the β structure is better than in the ASA, but this calculation still does not reproduce the observed transition pressure sequence. The reason is that the two-panel calculation for Sn underestimates the effects of the hybridization between the 4*d* states and the top of the 5*p* band. One should therefore rather include the 4*d* states in the same panel as the 5*p*'s. Doing that, we obtain an α-β-bct-bcc *sequence* that is consistent with experiment, but the minima of the total-energy curves are far too far apart. This follows from Fig. 6(b). The calculated transition pressures are therefore too high. The minimum α-phase energy is now 5.1 mRy below that of β-Sn. The pseudopotential calculations[14] predict this energy difference to be 2.5 mRy, still too large when the relative stability (Sec. I) of the two phases is considered. It appears that the one-panel LMTO calculation *overestimates* the effects of hybridization to the 4*d* states. This is a result[33] of the LDA which yields too high lying 4*d* states due to incomplete cancella-

tion of the self-interaction in the exchange term for these very localized states. We do not perform a complete self-interaction corrected (SIC) (Refs. 34 and 35) calculation, but decided rather to simulate the small changes in the total energies by performing the LDA calculation with the 4*d*'s somewhat downshifted. Thus, we do not include a SIC potential. Therefore, the shift that has to be applied to the 4*d* energies is given by the orbital exchange-correlation energy corrections, $\delta_{\alpha\sigma}$, as defined in the work by Perdew and Zunger.[34]

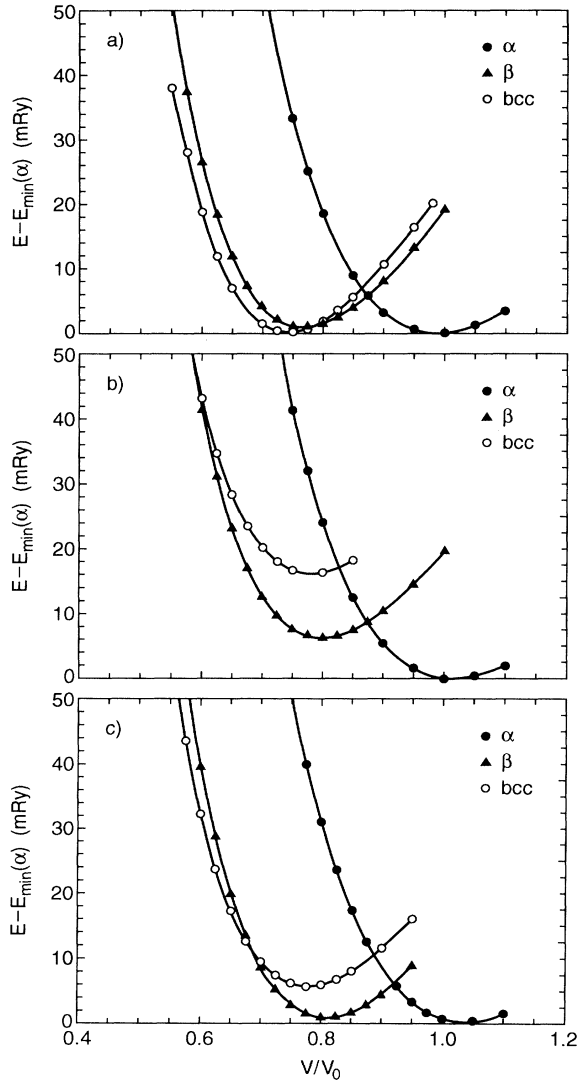

FIG. 6. Total energies (per atom) as functions of volume (per atom) calculated by means of the full-potential LMTO method for α-, β-, and bcc-Sn. V_0 is the observed equilibrium volume for α-Sn. (a) represents a two-panel calculation where the 4*d* states are calculated in the lower-energy panel, and where the upper panel couples to essentially the 5*d* states (see text). In (b) the 4*d*'s are included in the same valence-band panel as the 5*p*'s, i.e., the band structure calculations use only one panel. The results in (c) are obtained from a calculation like that in (b), except for the fact that the 4*d* states have been downshifted by 1.5 eV. The total energies are in all cases given relative to the minimum in the α phase.

The order of magnitude of the shift can be obtained simply by integrating the orbital density, $n_{\alpha\sigma}(\mathbf{r})$:

$$\delta_{\alpha\sigma} \approx 0.2 \int n_{\alpha\sigma}(\mathbf{r})^{4/3} d\mathbf{r}(\mathrm{Ry}) \ .$$

Using a spherically symmetrized density, the crude estimate yields $\delta_{4d} \approx 2$ eV, and we have chosen to downshift the 4*d*'s by 1.5 eV. Other choices were examined also. A 2-eV shift gives essentially the same results as those obtained with 1.5 eV, whereas downshifting the 4*d*'s by 3.0 eV appears to overestimate the correction. A detailed fitting procedure is not necessary.[33] The expression above is also used to estimate the volume dependence of the correction. Due to the strong localization this is very small. We find

$$d \ln \delta_{4d} / d \ln V \approx 4 \times 10^{-3} \ ,$$

and we can therefore use a volume-independent shift in the pressure range considered here. The downshift of the 4*d* states by 1.5 eV is accomplished by redefining the $E_\nu(d)$ values in each iteration. This does not affect the total energy differences calculated for the high-pressure phases, but leads to an α-Sn energy curve that has its minimum 0.7 mRy below that of β-Sn, and simultaneously the bcc- and bct-total-energy minima are lowered with respect to those of α- and β-Sn. This is seen in Fig. 6(c).

The more detailed study of the pressure-induced transitions presented in Sec. III is based on calculations of the latter type, i.e., the one-panel FP-LMTO with the 4*d* states included as valence-band states, but downshifted by 1.5 eV (110.25 mRy). Since the calculations in this way do contain a feature of arbitrariness, we do not attempt to include the SO corrections, estimated above, and we also neglect corrections to the total-energy differences due to different zero-point motion energies of the various structures (except for the $\alpha \rightarrow \beta$ transition, where we make an estimate of this contribution). The core-state shift does not affect the optimization of the c/a ratios for the bct and β phases.

III. PRESSURE-INDUCED TRANSITIONS

Total energies $E(V)$ were obtained from self-consistent LMTO calculations for 16–23 different volumes (V) for the α phase, the β-Sn with c/a ratios 0.52, 0.53, 0.54, 0.5518, and 0.56, respectively. The bct structure was similarly calculated for a range of c/a: 0.85, 0.88, 0.89, 0.90, 0.91, 0.92, 0.93, 0.95, 0.98, 1.00 (bcc), 1.02, and 1.04. Also, in order to examine a possible bcc$\rightarrow$fcc transition, a series of calculations were made for $c/a > 1$, choosing the values 1.12, 1.20, 1.25, 1.30, 1.35, $\sqrt{2}$, 1.45, and 1.50. The c/a ratio $\sqrt{2}$ makes the bct structure identical to fcc. The hcp structure was also examined over a range of c/a values allowing an optimization at each pressure value. For each of these structures the energy-volume relation was obtained by a least-squares fit to six functions of volume (V): $V^{-2n/3}$, $n = 0, \ldots, 5$. From these fits pressures (P) and bulk moduli (B_0) vs V were deduced. Interpolation on a fine grid was then used

to calculate Gibbs free energy at zero temperature, the enthalpy $H(P)$ as a function of the theoretical pressure. The structure that at a given pressure has the lowest enthalpy is the one that is stable (at $T=0$). The α structure was studied for pressure up to 600 kbar, whereas the others were followed to 2 Mbar.

The calculated properties of nine Sn phases at zero pressure are listed in Table I (where we also compare to some experimental data[36–38]). The theoretical equilibrium volume for α-Sn is 3% too large,[39] and therefore the calculations yield a theoretical bulk modulus, i.e., B_0 calculated at the theoretical equilibrium volume, that is smaller (447 kbar) than measured (530 kbar). The theoretical value of B_0 at the experimental volume is 509 kbar, i.e., in good agreement with the experiment of Ref. 38. The value, 512 kbar, obtained in Ref. 14 for the bulk modulus appears to agree better with experiment than ours, but that result was obtained[14] at a volume that is too small, $V/V_0=0.962$.

The equilibrium volume of β-Sn is found to be 20% smaller than that of the α phase, in good agreement with observations. Our calculated equilibrium volume for β-Sn is 2% larger than observed. The pseudopotential calculation[14] yielded a volume that is 6% too small. The axial ratio c/a obtained by minimizing the total energy for β-Sn is 0.541, in good agreement with experiment,[40] 0.546, as well as the calculation of Ref. 14, 0.545. The pseudopotential calculation by Corkill, García, and Cohen[13] yielded the value 0.546. The Sn atom at the origin (0,0,0) has four neighbors at $(\pm a/2,0,c/4)$ and $(0,\pm a/2,-c/4)$ and two neighbors at $(0,0,\pm c)$. In an "ideal" β structure these six atoms will all be nearest neighbors, i.e., the coordination number is exactly 6. Setting the distances equal, the "ideal" c/a ratio is therefore $(\frac{4}{15})^{1/2}=0.5164$. The actual β-Sn structure thus differs from the "ideal" one, and theory and experiment agree with respect to the deviation. The calculations further show (Fig. 7) that the c/a ratio does not change when pressure is applied.

Since we wish to calculate the pressure dependence of the phonon frequencies (Sec. IV), we must ensure that our theoretical $T=0$ isotherm (P-V relation) agrees sufficiently well with its experimental counterpart. Figure 8 shows a comparison between the theory and a Murnaghan equation with $B_0=520$ kbar and $B_0'=4$. These parameters result from the Murnaghan regression with B_0' constrained to 4 for β-Sn at 25 °C using a large data base (see Ref. 7, Table 4). The largest difference between theory and the fit to experiments, Fig. 8, is 3 kbar in the range 0–100 kbar, the pressure range in which the β structure exists.

Table I also lists the calculated minimum total energies, E_0, all relative to that of the α phase. It is seen that E_0 for bct with $c/a=0.90$ is lower than E_0 for bcc-Sn. Although the equilibrium volumes ($V/V_0=0.778$ and 0.776) are the same within computational accuracy, this does not exclude that, with increasing pressure, Sn *first* transforms to bct and later to the bcc structure. The P-V curves increase more rapidly with P in bct than bcc, a fact that is also reflected in the larger bulk modulus of bct-Sn than of the bcc structure at equilibrium (Table I).

The main results of the calculated pressure-induced structural transitions are summarized in Fig. 9 showing the enthalpies of the α, β, and a bct phase ($c/a=1$ is

TABLE I. Sn. Zero-pressure properties. V_0 is the experimental equilibrium volume per atom of Sn in the α phase. It corresponds to a lattice constant $a_0=6.483$ Å (Ref. 36). The table lists the equilibrium volumes V, bulk moduli B_0 (in kbar) for nine structures, and the axial ratios c/a. The bulk moduli are calculated at the theoretical equilibrium volumes, but in two cases we also give (in parentheses) the values calculated at the observed equilibrium volumes. E_0 is the minimum total energy (in mRy per atom) with the α structure as reference. "calc." refers to the present FP-LMTO calculation. The c/a ratios for the β-, bct-, and hcp structures were calculated (total-energy minimization), but those for phex and dhcp were chosen without detailed optimization.

	V/V_0	B_0 (kbar)	c/a	E_0 (mRy)	
α	1.030	447 (509)		0.000	calc.
	1.000[a]	530[b]			expt.
β	0.801	544 (593)	0.541	0.719	calc.
	0.784[c]	579[c] 549[d]	0.546[e]		expt.
bct	0.778	520	0.90	5.052	calc.
bcc	0.776	497		5.594	calc.
fcc	0.791	508		5.262	calc.
sc	0.842	484		7.071	calc.
hcp	0.783	616	1.628	4.808	calc.
dhcp	0.788	517	3.266	5.220	calc.
phex	0.818	500	1.000	6.215	calc.

[a]Reference 36.
[b]Reference 38.
[c]Reference 37.
[d]Reference 4.
[e]Reference 40.

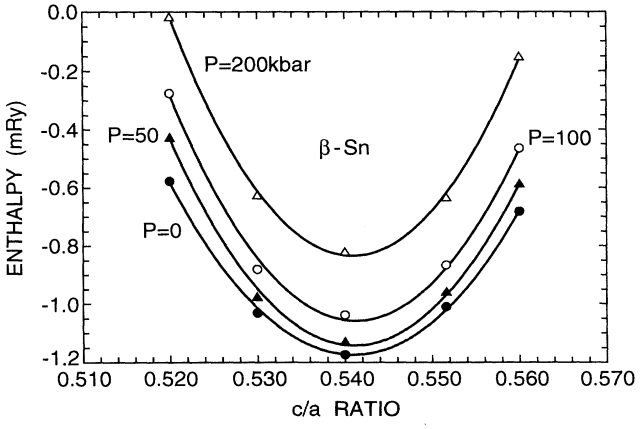

FIG. 7. Calculated free energy ($T=0$ K) of β-Sn at four different pressures, 0, 50, 100, and 200 kbar, as functions of the axial ratio, c/a. Symbols represent the calculated values, the curves second-order least-squares fits. Within the accuracy of the calculation no change with pressure is found for the c/a value corresponding to the energy minimum.

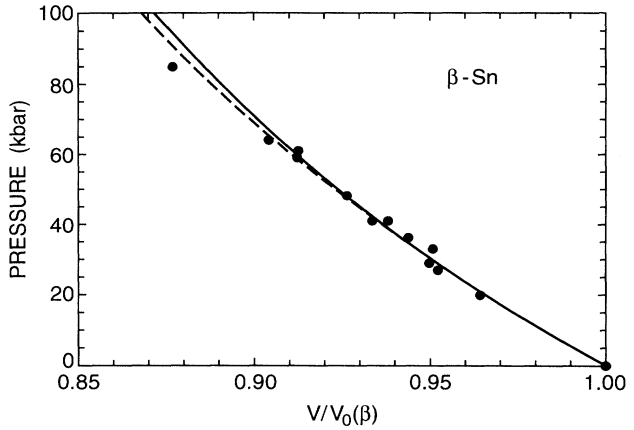

FIG. 8. Zero-temperature isotherms of β-Sn, pressure P vs volume P [normalized by the β-phase equilibrium volume, $V_0(\beta)$]. The full line represents the present theory, dashed a Murnaghan fit to experiments (see text), and the points are the "raw" experimental data from Ref. 7.

chosen here). The calculation shows that the $\alpha \rightarrow \beta$ transition should occur at 2 kbar, and the $\beta \rightarrow$bct at 104 kbar. The latter will be examined in more detail below, but this first result is close to the experimental value of the transition pressure, 95 kbar, obtained[6] at *room* temperature. The experimental transition pressure at $T=0$ K is estimated to be ≈ 130 kbar, or slightly less, (see Sec. V). The $\alpha \rightarrow \beta$ transition pressure is very low, as one should expect. Its actual value, though, depends on zero-point-motion corrections, and at finite temperatures, of course on entropy contributions. The contribution to the total energy from the zero-point motion may be estimated as $E_0 = 9/8 k_B \theta_D$, where θ_D is the Debye temperature. Experimental[41,42] values of θ_D are for the α and the β phases 220 and 195 K, respectively (at zero pressure). The zero-point correction will, therefore, lower the energy minimum of β-Sn by ≈ 0.16 mRy with respect to

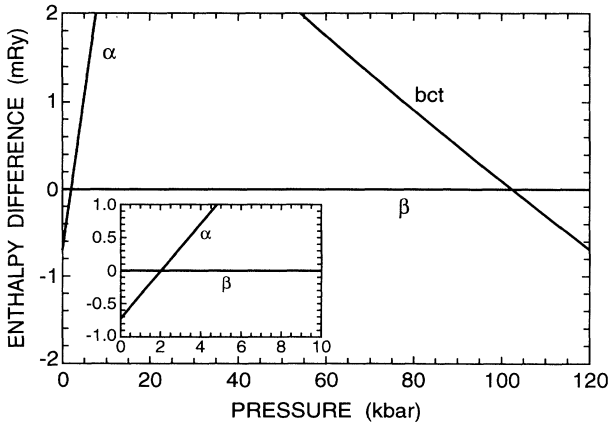

FIG. 9. Enthalpies for α-, β-, bct-Sn (bcc) vs (theoretical) pressure. The β phase is taken as a reference. The insert shows the regime close to $P=0$ on an expanded scale.

that of α-Sn. Still, the α phase has the lowest free energy at zero pressure and temperature.

The axial ratio of the β phase does not, as mentioned above, change within the pressure range where this structure is stable. But the bct structure, on the other hand, does change its c/a ratio when P is increased. In Figs. 10(a)–(c) we show how the calculated enthalpy at pressures ranging from 0 to 500 kbar varies with c/a. At $P=0$ [Fig. 10(a)] the optimized value of c/a is 0.90. Just at the transition pressure, $P=100$ kbar in Fig. 10(b), we find two minima in the enthalpy curve (note the similarity with the results in Ref. 14, Fig. 2, obtained for a somewhat more compressed lattice). At this pressure the slightly more stable bct structure ($c/a=0.91$) is separat-

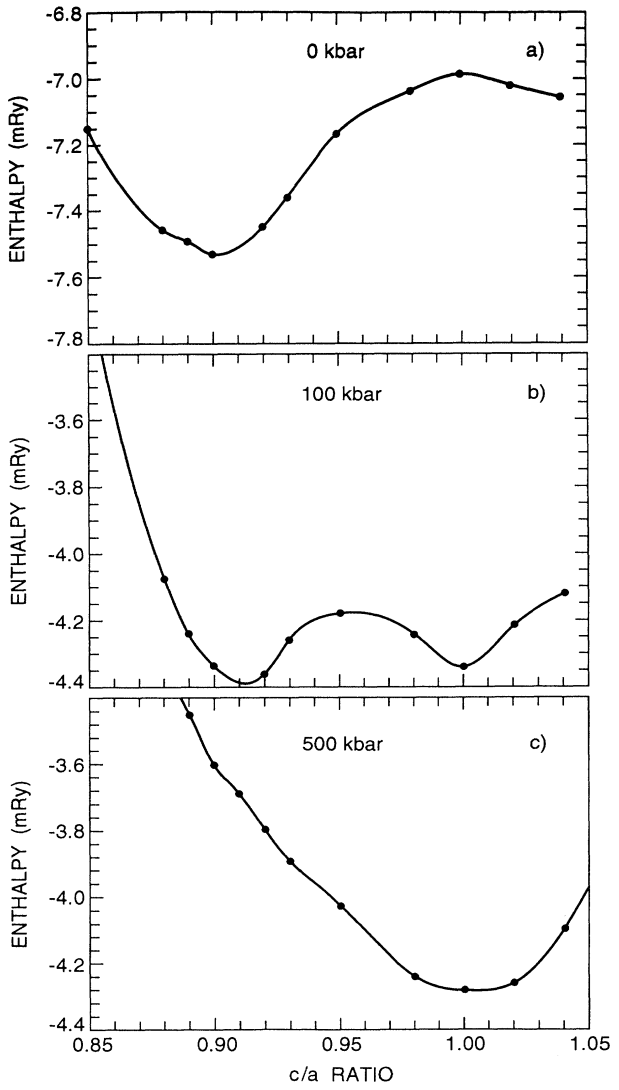

FIG. 10. BCT-Sn. Enthalpy vs axial ratio, c/a, at various pressures, P. (a) $P=0$; (b) 100 kbar; (c) 500 kbar. The curves (spline fit) are drawn through the calculated points marked, and serve only as a guide for the eye. The numerical scatter in the calculations is ± 0.02 mRy. The curves shown here do not have a common energy reference.

ed from the bcc minimum ($c/a=1.0$) by a small energy barrier, ≈ 0.2 mRy. This is, at room temperatures, much smaller than a thermal energy, ≈ 1.8 mRy, and we would therefore expect the "bct" phase of Sn to consist of a mixture of bct crystals with c/a ranging from maybe ≈ 0.85 to a value above 1.0. As the pressure is increased we find that the bcc minimum drops with respect to the one near $c/a=0.9$, and above 400 kbar we find only one minimum in the enthalpy versus c/a curves [Fig. 10(c)]. Thus, at finite temperatures Sn is for pressures above ≈ 100 kbar expected to have bct structures with c/a ratios covering a finite range. At high pressures the bcc structure ($c/a=1$) will prevail.

The calculations show that the transition (at $T=0$) from the bct to the bcc structure is not continuous. The c/a ratio does increase with pressure, but it can never be forced above[18] 0.96 without jumping abruptly to 1.00 (bcc). The calculated rate of increase of c/a in the bct phase is, close to $P=100$ kbar, $d(c/a)/dP=10^{-4}$ kbar^{-1}. The observed rate is almost twice as large at this pressure.[6] The simple model of Ref. 18 yields a pressure coefficient of c/a that is close to the result of the present full calculation.

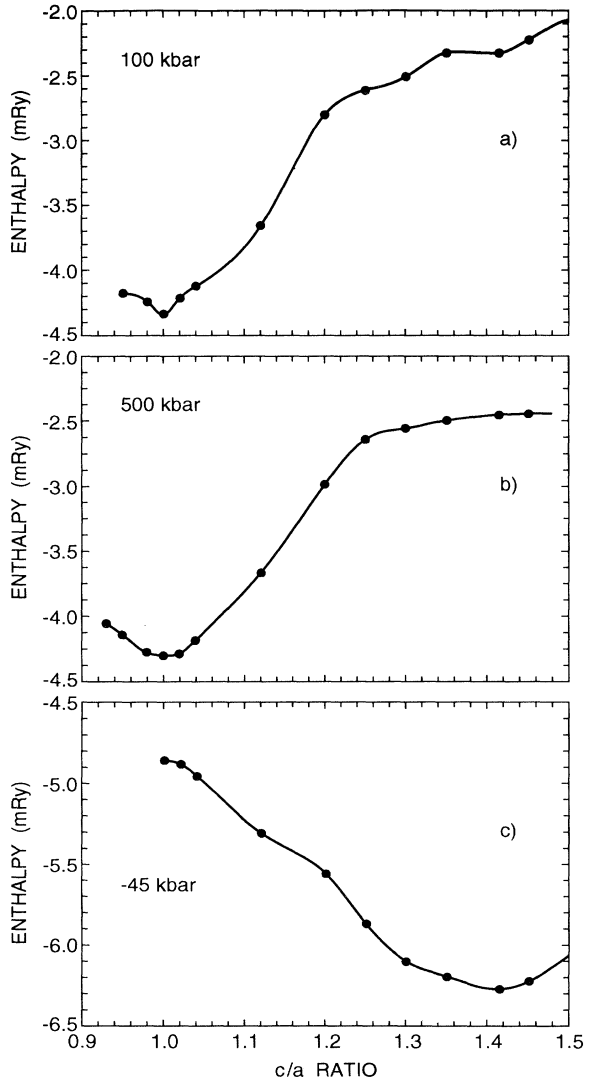

FIG. 11. BCT-Sn. Enthalpy vs axial ratio, $c/a>1$, at various pressures P. (a) $P=100$; (b) 500 kbar; (c) -45 kbar. $c/a=\sqrt{2}$ corresponds to the fcc structure.

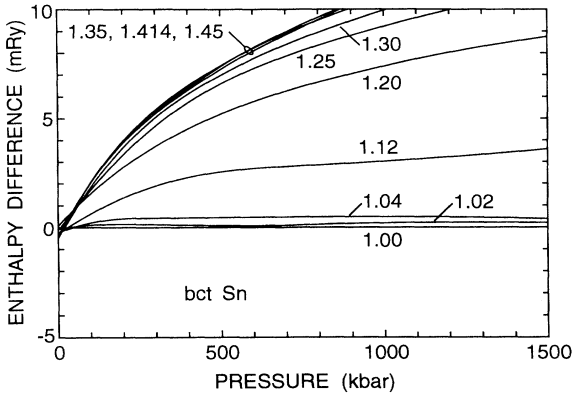

FIG. 12. Enthalpy differences, bcc-Sn is reference, for bct structures with different c/a ratios >1.0. (The calculation was, for $c/a=1.00$, 1.02, and 1.04 extended to 2 Mbar, but the enthalpy for $c/a=1.00$ remains the lowest.)

The calculations were extended to $c/a>1$ as illustrated in Fig. 11. A weak local minimum in the free energy is found for $c/a=\sqrt{2}$, the fcc structure, but there is no positive value of the pressure for which fcc-Sn would have a lower energy than bcc-Sn. Rather [see Fig. 11(c)] a slight expansion is needed to make fcc more stable. Figure 12 summarizes the free-energy calculations of bct-Sn for c/a ratios above 1.00 (bcc). The bcc structure remains stable up to very high pressures against tetragonal distortions.

The hexagonal close packed (hcp) structure of Sn was examined as well. The axial c/a ratio varies slightly with pressure (Fig. 13). Our calculations predict that the c/a ratio in the hcp phase should be slightly smaller than the ideal 1.633, whereas Ref. 13 suggests that it should be between 1.63 and 1.65. In Fig. 14 we show the calculated

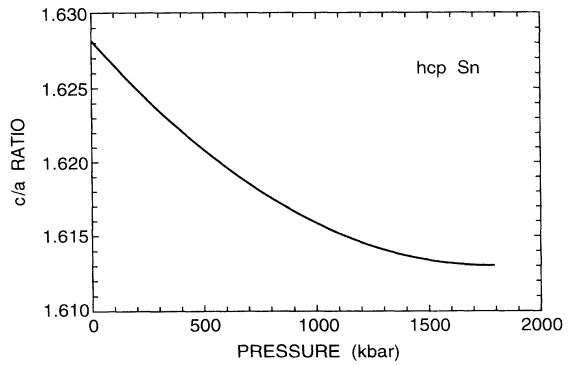

FIG. 13. Hypothetical hcp structure of Sn: Total-energy optimized c/a ratio versus (calculated) pressure.

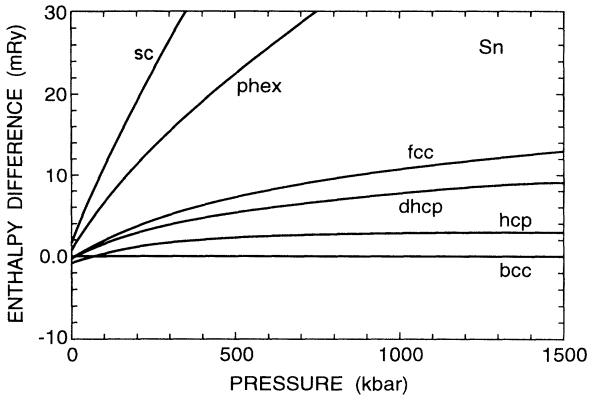

FIG. 14. Calculated enthalpies of bcc, fcc, hcp, sc, and dhcp phases of Sn as functions of pressure. The bcc phase has been taken as a reference.

enthalpies of simple cubic (sc), primitive hexagonal (phex), fcc, hcp ($c/a=1.63$ chosen here), double-hexagonal close packed (dhcp) phase of tin, all relative to bcc-Sn. It follows that no high-pressure transition from bcc to any of these other structures is predicted (actually, the calculations covered pressures up to 2 Mbar).

IV. Γ_3 and Γ_5 PHONONS IN β-TIN

In this section we describe the calculation of the optical-phonon frequencies of β-Sn in the long-wavelength limit, and the results are compared to those obtained by inelastic neutron scattering[43] and to recent Raman measurements.[8] At the Brillouin zone center the modes are of Γ_3 and Γ_5 (doubly degenerate) symmetry, respectively. Details of the symmetry properties are given in Ref. 44.

The phonon frequencies are derived from "frozen-phonon" calculations, i.e., a series of distortions (u) consistent with the symmetry of the mode considered are introduced, and the total energy calculated. For each of the modes we chose seven distortions, all displacements being less than 1% of the lattice parameter a. For each of these distortions we calculated the total energies for 18 volumes, yielding for each distortion $E(V,u)$ and $P(V)$ relations using the least-squares fitting described in the preceding section. The phonon frequencies as functions of V are subsequently derived by making a polynomial fit in u to $E(V,u)$. The coefficient of the second-order term yields the frequency.

The calculated frequencies are at $P=0$, $\nu(\Gamma_3)=45$ cm^{-1}, and $\nu(\Gamma_5)=130$ cm^{-1}, respectively. These are both higher than determined by the Raman experiment,[8] 42.44 and 126.60 cm^{-1}, but slightly lower than the neutron scattering results,[43] 46.5 and 132.5 cm^{-1}. The calculated pressure dependence of the phonon frequencies is compared to the Raman results in Fig. 15. An excellent agreement is found, although the sublinearity of the Γ_5 mode is somewhat weaker in the theory than the experiment. It was found that, within experimental error, the pressure dependence could be expressed (with P in kbar and ν in cm^{-1}) as[8]

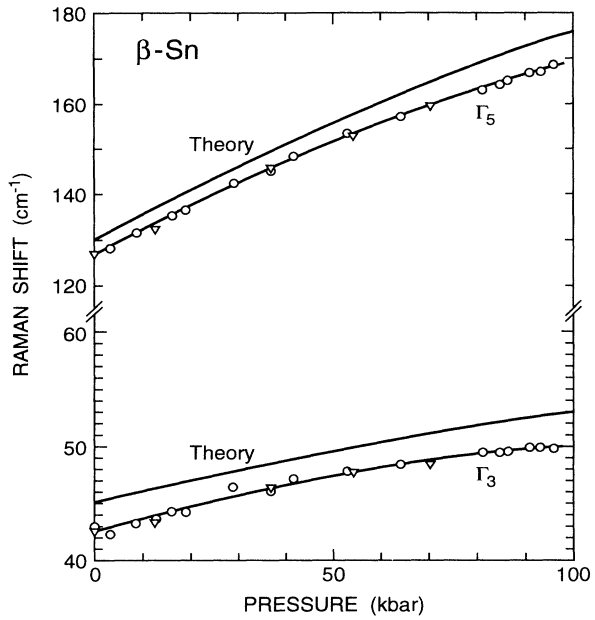

FIG. 15. Frequencies of the Γ_3 and Γ_5 phonon modes in β-Sn. Data points (and fitted curves) are from the Raman experiment of Ref. 8. The present theoretical results are shown by the curves without data points.

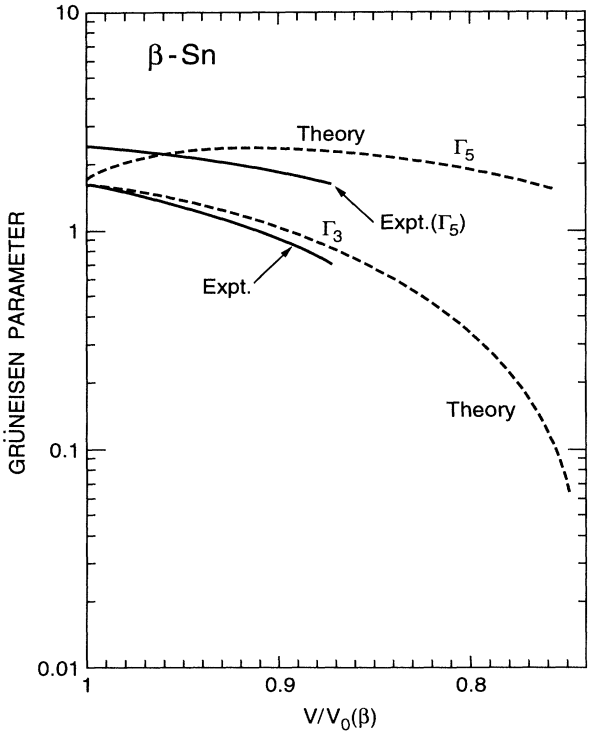

FIG. 16. Mode Grüneisen parameters of the Γ_3 and Γ_5 phonons in β-Sn. Full lines: Experiment (Ref. 8); dashed: present calculation. Volumes V are normalized by the experimental equilibrium volume $V_0(\beta)$ of β-Sn.

$$\nu(\Gamma_3)=42.44+0.1179P-0.436\times10^{-3}P^2 ,$$

$$\nu(\Gamma_5)=126.60+0.5517P-1.219\times10^{-3}P^2 .$$

Similar fits made to the calculations yield

$$\nu(\Gamma_3)=45.08+0.1460P-0.538\times10^{-3}P^2 ,$$

$$\nu(\Gamma_5)=129.90+0.5349P-0.512\times10^{-3}P^2 .$$

The mode Grüneisen parameters were also calculated, and in Fig. 16 we compare to the results obtained[8] from the Raman experimental data. The agreement is best for the Γ_3 mode. Theory predicts that the Grüneisen parameter for Γ_3 for very large compressions will go negative, but the pressure where this would occur is way beyond the $\beta\rightarrow$bct transition, 95 kbar (where the experimental data in Fig. 16 end). Such behavior has been found[8] in the β-Sn phase of Ge.

V. CONCLUSIONS

We have performed theoretical calculations, using the density functional theory, of the structural properties of tin under pressure. They yield the correct transition sequence, $\alpha\rightarrow\beta\rightarrow$bct$\rightarrow$bcc. Neither fcc nor hcp structures are expected as stable phases even at very high pressures. The calculated transition pressures agree well with experiments, and so do the optimized axial ratios (c/a) for the β and bct structures. The calculated pressure coefficient for c/a in the bct structure is smaller than observed, but it has the correct sign. The smallness of the energy barrier between bct-Sn with $c/a=0.9$ and the bcc structure suggests that at room temperature a range of c/a values should be observed for the bct phase. This was observed,[6] but mainly at the high end of the pressure range in which bct is found. At $T=0$ and $P\approx105$ kbar the calculation predicts the structure to be bct with $c/a=0.91$ (as observed, Ref. 6). The transition pressure obtained in Ref. 14 is higher, 190 kbar. Corkill, García, and Cohen[13] find an even larger value, 250 kbar, but estimate the zero-point vibrations to reduce the theoretical transition pressure to ≈235 kbar. A value larger than the 95 kbar as measured[6] at room temperature is indeed expected at $T=0$ K, which is most relevant for comparison to the calculations. From the phase diagram in Ref. 7 we estimate the "experimental" transition pressure to be ≈130 kbar (an upper limit, in fact) at zero temperature. The data in Ref. 7 agree with the experiment of Ref. 6 at room temperature. The zero-point motion contribution needs to be calculated, but if we assume that the estimate of the correction made in Ref. 13 is realistic, we conclude that the errors in the calculated transition pressure are similar, concerning magnitude, in Ref. 14 and our work (but the signs are opposite). An estimate based on the earlier phase diagram of Sn presented by Jayaraman, Klement, and Kennedy[45] suggests that the transition at $T=0$ K to the Sn-II phase should occur between 170 and 190 kbar. This would agree very well with the theory of Ref. 14, but, on the other hand, the room-temperature value of the transition pressure used in Ref. 45 appears to be too high, 113–115 kbar, measured by Jamieson.[45,46] The calculation of Ref. 13 predicts that c/a varies from 0.87 to 0.90 for pressures between 100 and 500 kbar. These c/a values are slightly smaller than our results and those measured.

The reason why β-Sn does not transform directly into the bcc structure was explained elsewhere[18] as being related to the splitting of the H_{15} level just below the Fermi level when a tetragonal strain is applied to bcc-Sn. In bcc-Sn the triply degenerate H_{15} (p_x,p_y,p_z) state is occupied, but the strain along $\hat{z}$ splits it into (p_x,p_y) and p_z. The latter moves above the Fermi level, and the electrons left over from its depopulation are redistributed over s-p states at E_F (which then increases slightly). The energy gained by this level splitting is opposed in part by a shift in the center-of-gravity of the p_x, p_y, and p_z states. In a "frozen-potential" approach it is the competition between these two one-electron energy changes that determine the relative stability of the bct and bcc structures as well as the value of c/a in bct-Sn.[18] By means of adjustment of one single parameter the simple model could be tuned to yield accurate numerical values of c/a and the bct$\rightarrow$bcc transition pressure. This model yielded a pressure coefficient for c/a close to the one obtained from the full calculation here, i.e., still smaller in magnitude than observed.

The pressure-volume relation (the $T=0$ isotherm) of β-Sn is in close agreement with experimental data, and the zone-center optical phonon modes vary with pressure in excellent agreement with recent Raman measurements.

The actual calculations were performed by means of the full-potential version of the LMTO method. It has been demonstrated that the simplest version of the LMTO, the atomic-sphere-approximation (ASA), is not sufficiently accurate for calculating some of the tiny total-energy differences. It is interesting, though, to observe that errors in the ASA total energies in several cases are quite small, and for bct-Sn even ASA predicts local minima close to $c/a=0.9$. In this phase of Sn the major ASA error occurs for c/a near 1.0 (bcc) where it fails to yield proper lattice stability. This error is associated with the improper calculation of the electrostatic interactions in the outer parts of the atomic spheres when spherically symmetrized charge densities are used.[27,47] The fact that ASA yields the (meta)stability of the bct structure near $c/a=0.9$ reflects that this feature is energetically favored by a minimum in the one-electron energy sum alone. This is consistent with the applicability of the simple model of Ref. 18 (the band structure).[32]

An extension of the calculations to include atomic and dynamic properties to tin oxides (SnO and SnO_2) will be presented elsewhere.[48] Also in those cases agreement with phonon frequencies is found for several modes observed by Raman spectroscopy.

ACKNOWLEDGMENTS

Discussions with A. Svane, E. Peltzer y Blancá, and C. O. Rodriguez have been very useful, and H. Olijnyk is thanked for communicating his Raman data prior to publication. A part of the computational work was carried out at the Höchstleistungsrechenzentrum für Wissenschaft und Forschung (HLRZ) in Jülich, Germany.

*Also at Max-Planck-Institut FKF, D-7000 Stuttgart 80, Germany.
[1]P. W. Bridgman, Proc. Am. Acad. Arts Sci. **74**, 425 (1942).
[2]W. Paul, J. Appl. Phys. **32**, 2082 (1961).
[3]J. D. Barnett, V. E. Bean, and H. T. Hall, J. Appl. Phys. **37**, 875 (1966).
[4]S. N. Vaiyda and G. C. Kennedy, J. Phys. Chem. Solids **31**, 2329 (1970).
[5]J. Staun Olsen, B. Buras, L. Gerward, and S. Steenstrup, J. Phys. E **14**, 1154 (1981).
[6]H. Olijnyk and W. B. Holzapfel, J. Physique (Paris) Colloq. **45**, Suppl. 11, C8-153 (1984).
[7]M. E. Cavaleri, T. G. Plymate, and J. H. Stout, J. Phys. Chem. Solids **49**, 945 (1988).
[8]H. Olijnyk, Phys. Rev. B **46**, 6589 (1992).
[9]M. A. E. A. Ament and A. R. de Vroomen, J. Phys. F **4**, 1359 (1974).
[10]J. Ihm and M. L. Cohen, Phys. Rev. B **23**, 1576 (1981).
[11]A. Svane and E. Antoncik, Solid State Commun. **58**, 541 (1986).
[12]A. Svane and E. Antoncik, Phys. Rev. B **35**, 4611 (1987).
[13]J. L. Corkill, A. García, and M. L. Cohen, Phys. Rev. B **43**, 9251 (1991).
[14]B. Cheong and K. J. Chang, Phys. Rev. B **44**, 4103 (1991).
[15]H. G. Salunke, G. P. Das, and N. E. Christensen, in *Proceedings of the XIII AIRAPT Conference, Bangalore, India, Oct. 1991* (Oxford & IBH, New Delhi, in press).
[16]N. E. Christensen, S. Satpathy, and Z. Pawlowska, Phys. Rev. B **34**, 5977 (1986).
[17]J. C. Phillips, *Bonds and Bands* (Academic, New York, 1973).
[18]N. E. Christensen, Solid State Commun. **85**, 151 (1993).
[19]S. Desgreniers, Y. K. Vohra, and A. L. Ruoff, Phys. Rev. B **39**, 10 359 (1989).
[20]O. K. Andersen, Phys. Rev. B **12**, 3060 (1975).
[21]M. Methfessel, Phys. Rev. B **38**, 1537 (1988).
[22]M. Methfessel, C. O. Rodriguez, and O. K. Andersen, Phys. Rev. B **40**, 2009 (1989).
[23]U. von Barth and L. Hedin, J. Phys. C **5**, 1629 (1972).
[24]N. E. Christensen, S. Satpathy, and Z. Pawlowska, Phys. Rev. B **36**, 1032 (1987).
[25]G. B. Bachelet and N. E. Christensen, Phys. Rev. B **31**, 879 (1985).
[26]D. Glötzel, B. Segall, and O. K. Andersen, Solid State Commun. **36**, 403 (1980).
[27]N. E. Christensen, Solid State Commun. **49**, 701 (1983).
[28]K. H. Weyrich, L. Brey, and N. E. Christensen, Phys. Rev. B **41**, 1392 (1988).
[29]A. T. Paxton, M. Methfessel, and H. Polatoglou, Phys. Rev. B **41**, 8127 (1990).
[30]H. G. Bekker and N. E. Christensen (unpublished).
[31]N. E. Christensen, Int. J. Quant. Chem. **25**, 233 (1984).
[32]The band structures used in Ref. 18 for the simple model explaining the occurrence of bct-Sn were in fact calculated within the ASA.
[33]It would also be desirable to examine the effect of including also the Sn-5*d* states in the basis, i.e., to use a basis set that is enlarged to include two types of *d* functions.
[34]J. P. Perdew and A. Zunger, Phys. Rev. B **23**, 5048 (1981).
[35]A. Svane and O. Gunnarsson, Phys. Rev. Lett. **65**, 1148 (1990).
[36]D. L. Price and J. M. Rowe, Solid State Commun. **7**, 1433 (1969).
[37]J. A. Rayne and B. S. Chandrasekhar, Phys. Rev. **120**, 1658 (1960).
[38]C. J. Buchenauer, M. Cardona, and F. H. Pollak, Phys. Rev. B **3**, 1243 (1971).
[39]Figure 6 shows that the equilibrium volumes for the α and β phases are calculated with two panels [6(a)] agree slightly better with experiments.
[40]R. W. G. Wyckoff, *Crystal Structures* (Wiley & Sons, New York, 1963).
[41]R. W. Hill and D. H. Parkinson, Philos. Mag. **43**, 309 (1952).
[42]W. S. Corak and C. B. Satterthwaite, Phys. Rev. **102**, 662 (1956).
[43]J. M. Rowe, Phys. Rev. **163**, 547 (1967).
[44]S. H. Shen, Phys. Rev. **163**, 532 (1967).
[45]A. Jayaraman, W. Klement, Jr., and G. C. Kennedy, Phys. Rev. **130**, 540 (1963).
[46]J. C. Jamieson, Science **139**, 762 (1963).
[47]N. E. Christensen, Phys. Rev. B **29**, 5547 (1984).
[48]E. L. Peltzer y Blancá, A. Svane, N. E. Christensen, M. S. Moreno, C. O. Rodriguez, O. M. Cappannini, and M. Methfessel (unpublished).